Photochemical & Photobiological Sciences (2023) 22:1825–1838
https://doi.org/10.1007/s43630-023-00413-5

ORIGINAL PAPERS

Insights into the phototautomerism of free-base 5, 10, 15, 20-tetrakis(4-sulfonatophenyl) porphyrin

Susanna Ciuti[1] · Angelo Carella[1] · Andrea Lucotti[2] · Matteo Tommasini[2] · Antonio Barbon[1] · Marilena Di Valentin[1]

Received: 13 February 2023 / Accepted: 21 March 2023 / Published online: 10 April 2023

Abstract

Phototautomerism in the excited states of free-base 5, 10, 15, 20-tetrakis(4-sulfonatophenyl) porphyrin (H_2TPPS^{4-}) has been investigated combining, for the first time, advanced Electron Paramagnetic Resonance (EPR) with fluorescence and Raman spectroscopy. Triplet EPR spectroscopy, performed in protic and deuterated solvents and in the presence of photoselection, confirms the occurrence of phototautomerization and additionally suggests the formation of the *cis* tautomer as a minor component. The zero-field splitting parameters and triplet sublevel populations indicate that the process is slow in the triplet state. The results obtained by EPR combined with photoselection and fluorescence anisotropy have been interpreted within a model which accounts for a fast *trans–trans* tautomerization promoted by a spin-vibronic coupling mechanism for intersystem crossing, with an even distribution of the two *trans* tautomers at liquid nitrogen temperatures for H_2TPPS^{4-}.

Graphical abstract

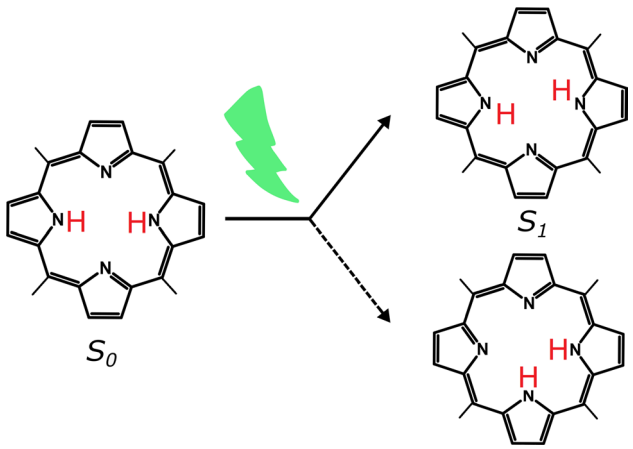

1 Introduction

Porphyrins are macrocycles with a central cavity that offers four nitrogen atoms and is open to coordination to a wide variety of metal ions. They are present in different classes of biologically active macromolecules, for example in the form of hemes, chlorophylls, or bacteriochlorophylls [1, 2]. Porphyrins are also valuable molecules in many fields within chemical and material science research, providing benefits for a variety of technological applications, for example in energy conversion [3] and non-linear optical materials [4].

Susanna Ciuti and Angelo Carella have contributed equally.

✉ Antonio Barbon
antonio.barbon@unipd.it

[1] Dipartimento di Scienze Chimiche, Università di Padova, Via Marzolo 1, 35131 Padova, Italy

[2] Dipartimento di Chimica, Materiali e Ingegneria Chimica, Politecnico di Milano, P.zza L. da Vinci 32, 20133 Milano, Italy

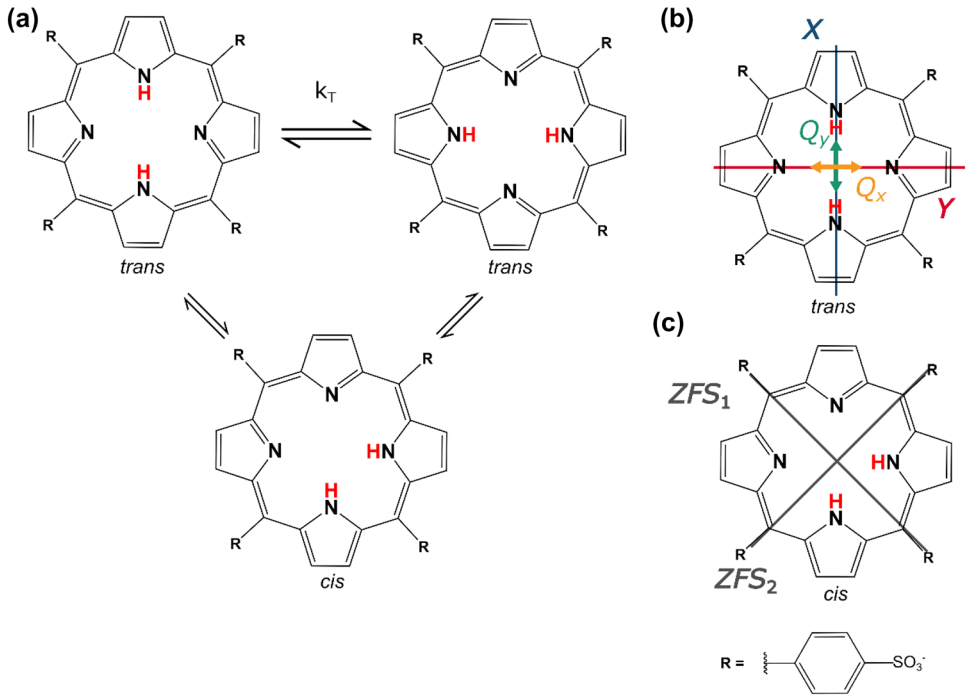

Scheme 1 **a** Molecular structure of free-base porphyrins and schematic representation of the trans-trans and trans-cis tautomerization processes; in the case of the free-base 5,10,15,20-tetrakis(4-sulfonatophenyl) porphyrin (H_2TPPS^{4-}) *R*= *p*-phenyl-SO_3^-, **b** orientation of the Q_x and Q_y transition dipole moments and the principal directions of the zero-field splitting (ZFS) axes (X and Y) taken from ref.s [6] and [7], under the assumption that $E<0$, for H_2TPPS^{4-} when no tautomerization takes place in the excited states, **c** orientation of the ZFS axes assumed for the cis tautomer in light of its molecular symmetry for H_2TPPS^{4-}

For these reasons, a wide and continuously expanding literature can be found on this class of biomolecules.

In the absence of a coordinated metal, the free-base macrocycle is doubly negatively charged and in the absence of substituents is named free-base porphine. This ion is stable in aprotic solvents or in protic solvents in basic conditions, while at neutral or acidic pH, two or four protons are bound to the internal nitrogen atoms and the macrocycle is either neutral or doubly positively charged [5]. The symmetry of the neutral porphine is D_{2h}, but rarely its derivatives can retain such a high symmetry; if non-linear substituents are symmetrically attached to the peripheral carbon atoms, the molecule possesses a C_2 axis or a mirror-symmetry element at most. In both situations, differently from the metalloporphines, the Q-bands are not degenerate.

The photophysics of the excited states of the porphine molecule and its derivatives is quite complex due to the presence of a series of states with rather close energy. The absorption spectrum, in the range between 400 and 650 nm, exhibits two groups of electronic transitions bands, labelled as Soret (400–450 nm) and Q-bands (500–650 nm), each characterized by two perpendicular transition dipole moments (TDMs) [6–8] and often displaying a series of vibronic progressions. In the case of the Q-bands, in molecules with symmetry lower than D_{4h}, two transition moments are present, Q_x and Q_y, normally ordered for increasing energy. Although the corresponding fundamental transitions and some vibronic progressions are visible, we wish to point out that the deconvolution of absorption bands at room temperature and high-resolution low-temperature Shpol'skii spectra show a number of different transitions contributing to them [9, 10], in line with DFT vibronic calculations. Nevertheless, for the two fundamental (0, 0) transitions and for the two different TDMs, we expect small, if at all, admixture with vibrational states [11].

The photophysics of porphine and its derivatives have been investigated by different groups, focusing on the excited singlet states. A series of basic and advanced spectroscopies like transient absorption and femtosecond fluorescence spectroscopy [12–14], also with pulse-train excitation [15], have been used. Zewail et al. and Kim et al. [12, 14] have shown that very fast relaxation mechanisms lead to the decay of the emission from hot states with typical times of 100–200 fs and, at the same time, the setting up of the fluorescence emission from the Kasha state occurs in less than 100 fs. The Kasha state is the one directly populated by excitation of the $Q_x(0,0)$ transition. While most of the fluorescence occurs from this state, emission from high energy states is detected as residual emission bands, due to fast intramolecular vibrational energy redistribution or solvent interactions inducing relaxation [12]. To gain knowledge about the fast dynamics in the excited singlet states, Waluk's group acquired the information on both steady-state and time-resolved fluorescence anisotropy of a free-base tetraphenylporphyrin (H_2TPP) upon photoexcitation of the different vibronic transitions of the Q-bands [13].

N–H tautomerism is a relevant process for the tetrapyrrolic structure of free-base porphyrins and it consists in the transfer of the inner protons of the macrocycle cavity among the four nitrogen atoms. In Scheme 1, we depict both the

trans–trans tautomerization, where both protons switch their position; the movement of a single proton, instead, produces a metastable *cis* tautomer [16]. The tautomerization occurring in the ground states of free-base porphine and in some analogues has been investigated in detail both in solution and in solid state by NMR techniques [16, 17].

So far, limited information is available for tautomerism in the excited states. The first evidence of a *trans–trans* phototautomerization was provided by Solov'ev et al. [18]. Phototautomerism has been invoked to interpret results obtained from optical spectroscopies: UV–Vis absorption [11], IR [19], fluorescence [20] and/or fluorescence anisotropy [21]. Phototautomerization has also been predicted theoretically [22], as result of the coupling of excited electronic states and vibrational modes. In chlorins, which are hydroporphyrines containing a partially reduced pyrrole group, beside the presence of the *trans–trans* tautomerization, also the *trans–cis* process has been documented [23]. Other porphyrin isomers have also been investigated by optical techniques [24]. Tautomerization in the photoexcited triplet state, which is populated by intersystem crossing (ISC) from the corresponding excited singlet state, has been studied by light-induced EPR techniques in porphycenes, which are tetrapyrrolic structural isomers of porphyrins, proving that the magnetic properties are sensitive probes if the process occurs in the EPR time scale [25, 26].

Although the intramolecular proton transfer is apparently without consequences for the molecule, tautomerization is a non-innocent process, as a change of the electronic distribution accompanies each proton jump. The impact of the *trans–trans* tautomerization on the molecular properties can be understood considering its equivalence with the rotation of the molecule (pseudorotation) by 90° [16, 19, 21]. This can have implications on several molecular aspects, like the transition dipole moment orientation [27] or the reactivity [28]. Therefore, it is mandatory to have clear information on this simple process which can happen in different electronic states.

In a recent report, we performed a comprehensive study of the triplet state of the free-base 5,10,15,20-tetrakis(4-sulfonatophenyl) porphyrin (H_2TPPS^{4-}) by combining light-induced advanced EPR techniques, best-suited for the triplet state investigation, and state-of-the-art computational methods. There, we interpreted some of the spectroscopic results as a consequence of the presence of an efficient phototautomerization [7]. Magnetophotoselection (MPS) experiments, realized by performing time-resolved EPR (TR-EPR) with excitation with linearly polarized light, were used to derive preliminary information on the process.

In the present work, we have examined in detail phototautomerism and its impact on the molecular properties of H_2TPPS^{4-}. To provide more solid evidence, MPS experiments have been performed in a deuterated solvent, enabling the exchange of the inner macrocycle protons to obtain D_2TPPS^{4-}, to slow down the exchange rate via the isotopic effect [29]. Furthermore, we have combined the EPR investigation with fluorescence anisotropy measurements to investigate at which stage phototautomerization occurs.

2 Materials and methods

2.1 Sample preparation

H_2TPPS^{4-} was purchased from Sigma Aldrich. Samples were obtained by dissolving the powder in the chosen solvent at a concentration of 60 μM, determined by optical absorption spectroscopy. Deuteration of the exchangeable central cavity protons (D_2TPPS^{4-}) in samples for TR-EPR spectroscopy was fulfilled by dissolving the powder in d_4-methanol (MeOD). Samples were degassed into quartz EPR tubes (3 mm i.d.) by freeze and thaw cycles and sealed under vacuum. The glass vitrification of the samples was obtained by flash-freezing samples in liquid nitrogen.

2.2 EPR measurements and data analysis

Experiments were recorded at X-band on a Bruker Elexsys E580 spectrometer, equipped with a 6.5 MHz preamplifier. The TR-EPR spectra were recorded in direct detection mode with the time traces sampled with a LeCroy 9360 oscilloscope. A Bruker ER 4117X-MD5 dielectric cavity inside a CF900 cryostat was used. The microwave power for the experiments was set at about 0.2 mW. The time resolution of the spectrometer was estimated to be less than 1 μs. Excitation was performed with an Nd:YAG laser (Quantel Rainbow) equipped with an optical parametric oscillator (OPO) pumped by the third harmonic module, with a 10 Hz repetition rate. Laser pulses were 5 ns long, with energies of 2–2.5 mJ/shot. MPS experiments were performed exciting the sample with linearly polarized light. The orientation of the polarization was controlled using a half-wave plate followed by a linear polarizer. Care was used to prepare transparent glasses without cracks. In a clear glass, the MPS effect is maximized, while a cracked and opaque glass favours scattering processes and, consequently, depolarization of light. Light linearly polarized either parallel (*par*) or perpendicular (*perp*) to the magnetic field was used. Consequently, molecules with the TDMs either parallel or perpendicular with respect to the magnetic field are prevalently excited in each mode. For an isotropic distribution of molecules in the ground state, the probability that a molecule is excited depends on the direction of the TDM ($\hat{\boldsymbol{u}}_{TDM}$, rigidly fixed in the molecular frame) and on the direction of the polarization of the light ($\hat{\boldsymbol{u}}_{E}$, fixed in the laboratory frame). Therefore, the excitation probability for

a single molecule as a function of its relative orientation is $p_{\omega,\varphi}^{par/perp}(\alpha,\beta,\gamma) = (\hat{\boldsymbol{u}}_{TDM} \bullet \hat{\boldsymbol{u}}_E)^2/N$, where N is a normalization factor and α, β, γ the Euler angles relating the laboratory and the molecular (ZFS) frame. We generally assume that the orientational distribution function is conserved after the ISC to the triplet state, which is valid if no processes (such as a tautomerization) alter the relative orientation between the molecular and ZFS frame. The shapes of TR-EPR spectra obtained exciting a transparent glassy solution with polarized light are thus altered with respect to the profile obtained with non-polarized, or isotropic, excitation: some components are reinforced, whereas others result reduced, depending on the relative orientation between the TDM and the ZFS axes. An insight on these aspects can be found in Ref.s [7, 30–32]. A careful reproduction of the lineshape of the TR-EPR spectrum obtained with light polarized parallel or perpendicular to the magnetic field allows the determination of the direction of the TDM with respect to the ZFS frame.

The experimental TR-EPR spectra as a function of the magnetic field were extracted at a fixed delay time of about 1.2 µs after pulsed laser excitation, near the maximum of the spectra intensity. TR-EPR data were then processed by subtracting the baseline offset before the trigger event. Isotropic spectra, corresponding to excitation with non-polarized light, were calculated as the sum $I_{par} + 2I_{perp}$, where I_{par} and I_{perp} are the EPR intensities obtained with light polarized parallel and perpendicular to the magnetic field, respectively, in analogy to optical polarization measurements [7].

Simulations were performed using a home-written MATLAB program for triplet powder spectra described in Ref.s [7, 30, 33]. The "esfit" routine [34] was employed to extract the best-fit parameters.

2.3 Optical emission measurements

Optical emission measurements were obtained either in cells or directly in the EPR tubes by using a FLS100 Edinburgh photoluminescence spectrometer equipped with polarizers. Excitation was obtained by a Xe lamp. For cooling of quartz cells, a Peltier plate was used near room temperature, while a quartz cold finger, filled with liquid nitrogen, allowed cooling to 77 K. H_2TPPS^{4-} was dissolved in a mixture (3:2) of ethanol/methanol and in non-protic solvents (dimethylformamide/2-methyltetrahydrofuran/dichloromethane and dimethylformamide /acetonitrile); D_2TPPS^{4-} samples were obtained by dissolving H_2TPPS^{4-} in MeOD; 2% of deuterated water was added to favour the formation of an optically clear glass.

Fluorescence anisotropy (r) was estimated at every wavelength of excitation from the ratio $r = \frac{GI_{vv} - I_{vh}}{GI_{vv} + 2I_{vh}}$, where I_{ij} refers to the intensity of emission with a given polarization of the excitation (i) and of the emission (j), while v and h stand for vertical and horizontal polarization, respectively. The experimental G-factor was automatically recorded from the spectrophotometer as $G = I_{hh}/I_{hv}$.

2.4 Raman measurements

The Raman spectra of H_2TPPS^{4-} and D_2TPPS^{4-} powders placed in sealed NMR tubes have been recorded with the Nicolet NXR9650 FT-Raman equipment (Nd-YVO4 1064 nm laser excitation, 4 cm^{-1} resolution, laser spot size 50 µm, power at the sample 1W). Density functional theory calculations of the off-resonance Raman spectra have been carried out with the B3LYP/6-31G (d,p) method by using the Gaussian software [35]. We have considered models of H_2TPPS^{4-} and D_2TPPS^{4-} interacting with Na^+ ions placed in correspondence of the four $-SO_3^-$ groups. To ease the comparison between experimental and simulated spectra, a uniform scale factor of 0.98 has been applied to the wavenumbers computed by DFT.

3 Results

In our previous work on the triplet state of H_2TPPS^{4-} in an ethanol:methanol 3:2 mixture, we found that, when performing MPS with linearly polarized laser excitation, the MPS effect of the triplet was reproduced with an apparent excitation of both the Q_x and Q_y bands with equal contributions, irrespective of the wavelength used; indeed, to simulate the MPS TR-EPR spectra an equal contribution to the orientational distribution function (see Materials and Methods) from the Q_x and Q_y TDMs was required [7]. This result was discussed in terms of a fast phototautomerism, in the EPR time scale, occurring in the excited singlet state, which provides the same distribution function as that obtained from excitation of both transitions. To gain further evidence and obtain a detailed description of the process, we decided to perform the EPR experiments in deuterated solvent and integrate the experimental findings on the triplet state with the investigation on the corresponding excited singlet state by optical spectroscopy. The purpose of using a deuterated solvent is to selectively exchange the central protons, potentially involved in phototautomerism, and to seek for the presence of an isotopic effect affecting the process.

We obtained TR-EPR spectra with photoselection for both H_2TPPS^{4-} and D_2TPPS^{4-} in an optically clear glassy solvent near liquid nitrogen temperatures. As a further step in the characterization, the molecules were photoexcited with polarized light at the maximum of each of the four visible Q-bands, labelled as $Q_x(0,0)$, $Q_x(0,1)$, $Q_y(0,0)$, $Q_y(0,1)$ (ordered by increasing energy, the electronic absorption spectrum is reported in Fig. S1). The aim was to detect

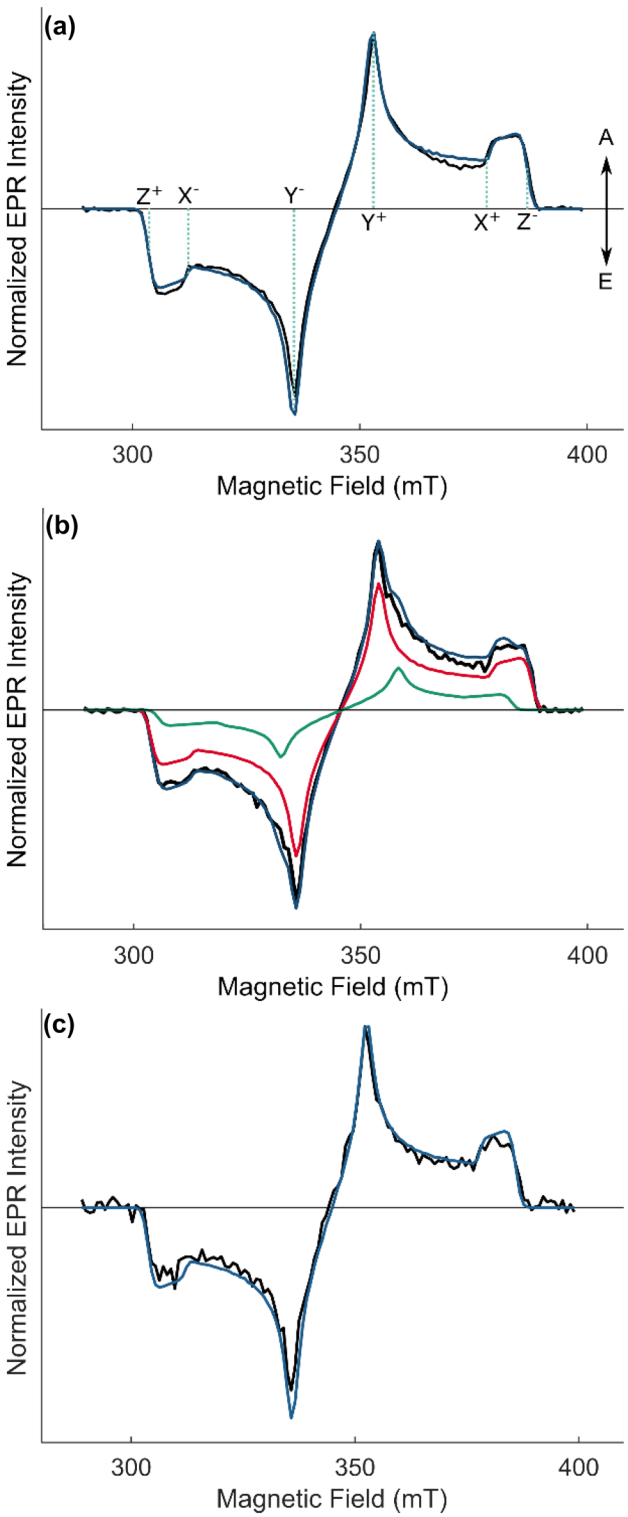

Fig. 1 **a** Isotropically excited TR-EPR spectrum of the triplet state of D_2TPPS^{4-} in deuterated methanol; **b** isotropically excited TR-EPR spectrum of the triplet state of H_2TPPS^{4-} in an ethanol:methanol 3:2 mixture; **c** isotropically excited TR-EPR spectrum of the triplet state of H_2TPPS^{4-} in an ethanol:methanol 3:2 mixture with the addition of KBr. Experiments were performed at X-band at 80 K, exciting at 640 nm, within the $Q_x(0,0)$ absorption band. Experimental data are shown in black and simulations are reported in blue; the two components that give rise to the H_2TPPS^{4-} spectrum simulation in (b) are shown in red (triplet 1) and green (triplet 2). Simulation parameters are reported in Table 1. The turning points of the spectrum (for $D>0$, $E<0$) are indicated. A = enhanced absorption, E = emission

possible differences in the MPS effects due to either the excitation of transitions with orthogonal orientation of the TDMs (see Scheme 1b) or in the presence of vibronic coupling, which could induce a reorientation of the TDMs [36].

Initially, we had to face a complication deriving from the difference between the isotropically excited TR-EPR spectra of H_2TPPS^{4-} and D_2TPPS^{4-} upon excitation on the lowest energy $Q_x(0,0)$ absorption band. The difference is better observed by inspection of the region between the X and the Y turning points of the triplet spectrum, as reported in Fig. 1a, b, and it cannot be reproduced by simulation by varying the ZFS parameters or the populations of the ZFS states upon deuterium exchange. We attribute this difference to the presence of a second minor species (triplet 2), beside the dominant triplet (triplet 1) characterized by an orthorhombic ZFS tensor [7, 37]. This triplet 2 is tentatively assigned to a *cis* tautomer based on various experimental evidence, i.e. the variation of the relative weight between the two triplets with the excitation wavelength, with isotopic substitution of the central protons and with external heavy atom effect on the weights. Additionally, the MPS behaviour of triplet 2 is in line with what is expected for a *cis* isomer. A detailed discussion is reported below.

Simulations using two triplet contributions gave a satisfactory fitting of the spectra and the parameters are reported in Table 1. The ZFS parameters and relative populations of triplet 2 differ from those reported in the literature for H_2TPPS^{4-}. By varying the excitation wavelength, in the case of H_2TPPS^{4-}, the triplet 2 contribution changes and becomes negligible when exciting on the $Q_x(0,1)$ and $Q_y(0,1)$ bands, while in the case of D_2TPPS^{4-}, triplet 2 is only observed when exciting on the $Q_y(0,0)$ transition and is characterized by a much lower intensity (see Fig. S2). We note that the presence of this second species has been found also in samples deriving from different preparation batches, with the same wavelength-dependent behaviour, and in a related parent molecule (H_2TPP, unpublished data), allowing us to exclude that this may depend on the presence of impurities.

To get an insight into the minor triplet component and its generation mechanism, we exploited the external heavy atom effect to enhance the ISC rate by adding a bromine salt to the solution of H_2TPPS^{4-} in a 1:100 ratio. The resulting isotropically excited TR-EPR spectrum on the $Q_x(0,0)$ band does not show any contribution from triplet 2, as reported in Fig. 1c. This has been found when exciting any of the four absorption bands (see Fig. S3). The final assignment of triplet 2 derives from detailed analysis of MPS, as described below.

Table 1 Simulation parameters for the TR-EPR spectra of H_2TPPS^{4-} and D_2TPPS^{4-} with isotropic light excitation: ZFS parameters $D = -3 \cdot Z/2$ and $E = (Y–X)/2$ (±5 MHz), relative populations of the triplet sublevels p_i (±0.01). For each band, k_n (±5%) is the weight of each of the two normalized triplet state spectra S_n in the simulation, obtained as $S = k_1 \bullet S_1 + k_2 \bullet S_2$

	|D| (MHz)	|E| (MHz)	p_X	p_Y	p_Z	k_n (%) $Q_x(0,0)$	k_n (%) $Q_x(0,1)$	k_n (%) $Q_y(0,0)$	k_n (%) $Q_y(0,1)$
H_2TPPS^{4-} 80 K									
Triplet 1	1182	227	0.30	0.63	0.07	75	100	80	100
Triplet 2	1100	120	0.38	0.55	0.07	25	0	20	0
D_2TPPS^{4-} 80 K									
Triplet 1	1182	227	0.27	0.63	0.10	100	100	95	100
Triplet 2	1100	120	0.38	0.55	0.07	0	0	5	0
D_2TPPS^{4-} 105 K									
Triplet 1	1182	227	0.27	0.63	0.10	/	/	/	100

MPS measurements provide the orientation of the TDMs in the ZFS tensor frame for the different excitation bands [30] and, in the case of free-base porphyrins, they allow precise investigation on phototautomerism, as demonstrated in ref. [7]. Figure 2 reports the TR-EPR spectra, obtained with linearly polarized light parallel and perpendicular to the magnetic field, with excitation in correspondence to the $Q_x(0,1)$ and $Q_x(0,0)$ bands, for both H_2TPPS^{4-} and D_2TPPS^{4-}. Analogous spectra obtained with excitation within the two Q_y bands are reported in Fig. S4. All the TR-EPR spectra with photoselection exhibit enhanced X and Y triplet features when linearly polarized light excitation is parallel to the magnetic field and enhanced Z transitions when it is polarized perpendicular to it.

Fitting of the EPR spectra with MPS was performed by fixing the triplet magnetic parameters and weights of the two triplet components, as derived from the simulation of the isotropically excited spectrum, while varying, only for triplet 1, the weights of the two TDMs (%TDM_{Qy} and %TDM_{Qx}). The orientation of the Q_y and Q_x TDMs was fixed parallel to the ZFS X and Y axes, respectively (see Scheme 1b), as derived from DFT calculations [7]. For triplet 2, in the hypothesis that it is a contribution from the *cis* tautomer, we fixed the direction of the TDMs at 45° (±10°) with respect

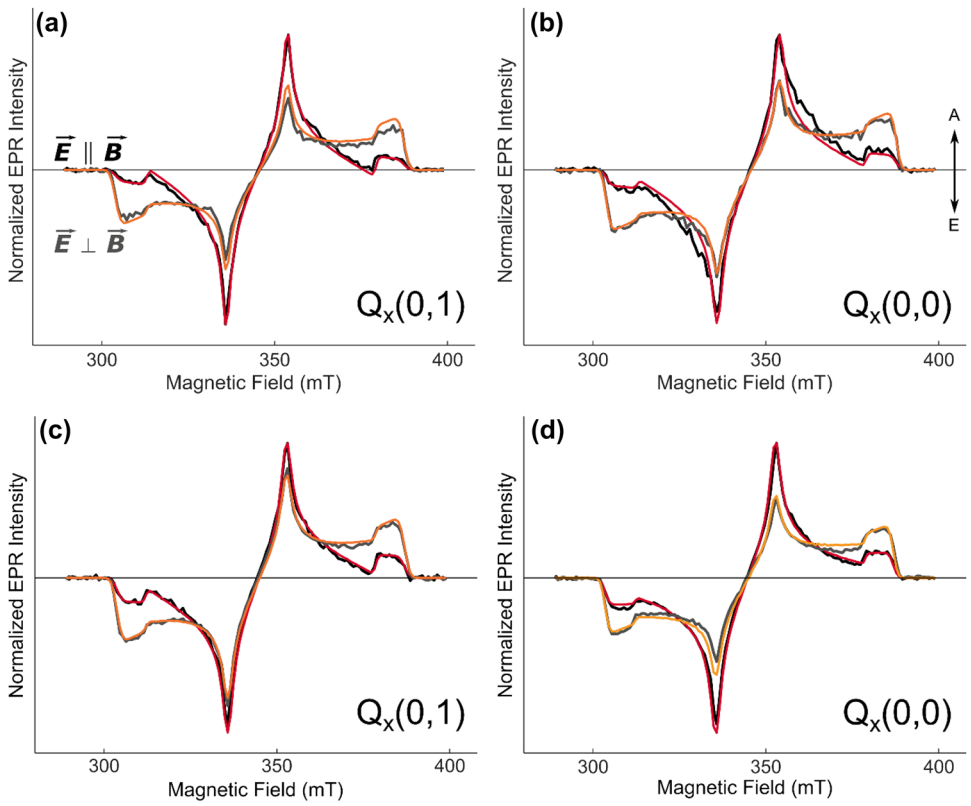

Fig. 2 Triplet state TR-EPR spectra of H_2TPPS^{4-} in ethanol:methanol 3:2 mixture (top, **a** and **b**) and of D_2TPPS^{4-} in deuterated methanol (bottom, c and d), exciting with linearly polarized light within the $Q_x(0,1)$ (left, **a** and **c**) and $Q_x(0,0)$ (right, **b** and **d**) absorption bands. Experiments were performed at X-band at 80 K. The spectra obtained with light polarized parallel and perpendicular to the magnetic field are reported, in black and grey, respectively; the corresponding simulations are shown in red and orange, in the same order. Simulation parameters are reported in Tables 1, 2. *A* enhanced absorption, *E* emission

to the in-plane X and Y principal directions of the ZFS tensor. The symmetry for *cis* is lowered from a D_{2h} to a C_{2v}, where the C_2 symmetry axis passes through two opposite *meso* carbon atoms. One of the principal axes of the ZFS-tensor is expected to be oriented along this C_2 symmetry axis, while the other principal axes are in the perpendicular plane. On the basis of the *cis* tautomer symmetry (see Scheme 1c), the corresponding ZFS tensor is rotated of 45° from the ZFS frame of the *trans* tautomers and both the Q_x and Q_y TDMs are oriented at 45° with respect to the in-plane principal directions since the absorption occurs in the *trans* conformation. The photoselected TR-EPR spectra have been nicely reproduced in this orientational frame and we can then assert that the triplet 2 spectral contribution is fully compatible with the *cis* tautomer. We cannot distinguish the formation as occurring in the singlet or in the triplet state. As from DFT calculations [22], the energy difference between the *cis* and *trans* forms is calculated to be 0.4 eV, on the other hand, the authors state that "the transfer of a single proton, which occurs in the lowest singlet excited state, is energetically more favourable than the concerted double proton transfer".

As already mentioned, in order to obtain a satisfactory fit of the triplet 1, contribution to the spectrum from both Q_y and Q_x TDMs were considered for excitation at all wavelengths. For H_2TPPS^{4-}, the weight of each component (%TDM_{Qy} and %TDM_{Qx}) is equal and it is conserved while changing the wavelength, whereas for D_2TPPS^{4-}, the relative contributions are not equal. It is worth noting that when exciting D_2TPPS^{4-} within the $Q_x(0,0)$ transition, the larger weight corresponds to TDM_{Qx}, and the analogous observation occurs for excitation within the $Q_y(0,0)$ transition for TDM_{Qy}. First of all, this implies that the TDM_{Qy} is oriented along the X ZFS axis and similarly, that the TDM_{Qx} is oriented along the Y ZFS axis, as obtained from DFT calculations (see Scheme1) [6]. Secondly, the different weight is compatible with a slowing down of the tautomeric process due to the isotopic effect. As for excitation within the other bands, the relative weights of the two contributions are also different, but in this case, the TDM orientation is not known and a reorientation of the TDM probably occurs, likely due to vibronic effects (see fluorescence anisotropy showing very different *r* values).

For each simulation, an orientational distribution function deriving from excitation of two TDMs have been used. The orientational axis was taken along the indicated principal direction of the ZFS ($D > 0$ and $E < 0$ have been assumed); $\%TDM_i$ (± 2) is contribution as a percentage relative to each TDM (see Scheme 1and Supporting Information). The simulations account for a small depolarization with a relative contribution of the isotropic contribution C_{iso} (%) (± 2).

The triplet spectra were recorded also at higher temperature to have indication of a possible thermal activation of the process. Figure 3 shows a comparison between triplet EPR spectra obtained for the D_2TPPS^{4-} with parallel and perpendicular excitation on the $Q_y(0,1)$ transition, at 80 K and 105 K. The corresponding simulation parameters are reported in Table 2. While at 80 K the ratio $\%TDM_{Qy}$: $\%TDM_{Qx}$ is 34:66, increasing the temperature leads to a ratio of 53:47 at 105 K, much closer to the even weight, that is found for H_2TPPS^{4-} at 80 K. We note that the magnetic parameters are not affected by the temperature and are indicative of the absence of an effective exchange between the two *trans* conformers within the triplet state. The most sensitive parameter is the ZFS parameter E, which should average to zero in the case of dynamical average of the in-plane X and Y triplet components: the ZFS tensor is orthorhombic and does not change in the temperature range under investigation.

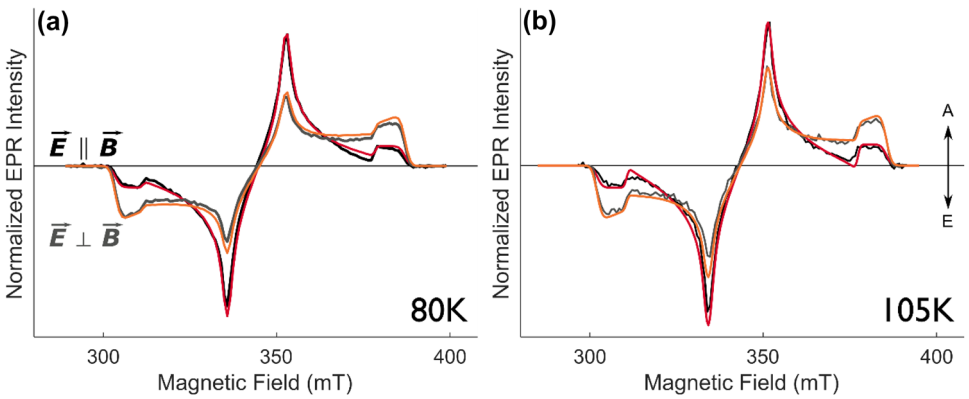

Fig. 3 Triplet state TR-EPR spectra of D_2TPPS^{4-} in deuterated methanol, exciting with linearly polarized light within the $Q_y(0,1)$, at 80 K (**a**) and 105 K (**b**). Experiments were performed at X-band. The experimental traces obtained with light polarized parallel and perpendicular to the magnetic field are reported, in black and grey, respectively; the corresponding simulations are shown in red and orange, in the same order. Simulation parameters are reported in Tables 1, 2. *A* enhanced absorption, *E* emission

Table 2 Parameters of the simulation for the main triplet component (triplet 1) of the TR-EPR spectra with magnetophotoselection effect and excitation within the four Q-bands

Excitation band						
	C_{iso} (%)		$Q_x(0,0)$	$Q_x(0,1)$	$Q_y(0,0)$	$Q_y(0,1)$
H_2TPPS^{4-} 80 K	10	$\%TDM_{Qy}$	50	50	50	50
		$\%TDM_{Qx}$	50	50	50	50
D_2TPPS^{4-} 80 K	24	$\%TDM_{Qy}$	34	54	65	36
		$\%TDM_{Qx}$	66	46	35	64
D_2TPPS^{4-} 105 K	24	$\%TDM_{Qx}$	/	/	/	47
		$\%TDM_{Qx}$	/	/	/	53

Further information on the process was sought performing experiments of both static and dynamic fluorescence anisotropy of the excited singlet state. To isolate the potential contribution to the depolarization due to phototautomerism, the effect produced by molecular reorientational motion was first considered. At room temperature, in some typical low viscosity solvents, the fluorescence anisotropy for H_2TPPS^{4-} was found to be practically zero as measured on the (0, 0) emission band at 650 nm (data not shown). This is expected for molecules with a fast orientational diffusion dynamics as compared with their lifetime (see Fig. S5 for the fluorescence decay of D_2TPPS^{4-} in deuterated methanol at room temperature and 77 K). Then, in order to get rid of the reorientational motion contribution, we dissolved H_2TPPS^{4-} in a viscous glycerol solution (with 10% of water was added in order to obtain an optically transparent solution) and cooled the system down to 255 K to obtain a rigid glassy matrix. The maximum value for the fluorescence anisotropy was obtained for the $Q_x(0,0)$ band ($r = 0.15$ at 255 K, see Fig. S6). As values of $r = 0.2 \div 0.3$ were previously found for parent porphyrins [38, 39] in a regime where motional depolarization should be ineffective, measurements at even lower temperatures (77 K) were performed in frozen glassy solutions, using different protic and aprotic solvents mixtures. Care was used to obtain optically transparent glasses and several attempts were conducted to verify the reproducibility of the results. In Fig. 4a, a representative example is displayed where the fluorescence anisotropy, detected at 650 nm, is reported as a function of the excitation wavelength. Positive r values are displayed for excitation on the Q_x vibronic bands: the maximum r value close to 0.25 for the $Q_x(0,0)$ transition, in agreement with the r value reported in the literature for H_2TPP [38, 39], a negative r value for excitation in correspondence of the $Q_y(0,0)$ band and a small positive value for the $Q_y(0,1)$ transition. Detection of the fluorescence anisotropy at 717 nm reveals analogous trends but characterized by generally lower values. Similar behaviour is displayed also in other selected solvent mixtures, with differences comparable with the noise level.

To gain further information, fluorescence anisotropy was also followed in time with excitation on the Soret band, where an anisotropy characterized by lower values is expected due to the scarce resolution of the different absorption bands. The signals, reported in Fig. 4c, show an

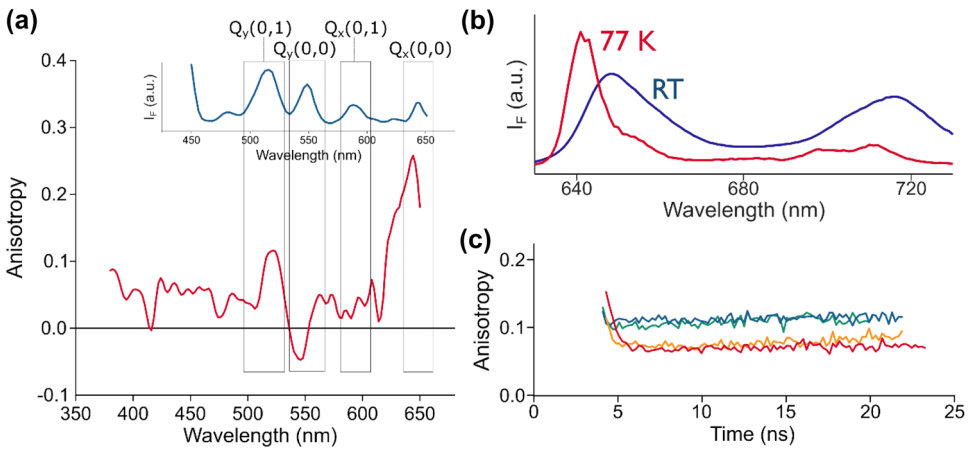

Fig. 4 **a** Fluorescence anisotropy at 77 K for H_2TPPS^{4-} in an ethanol:methanol 3:2 mixture detecting the emission at 650 nm (red). An excitation profile is provided for reference, with the attribution of the transition bands; **b** fluorescence spectra at room temperature and at 77 K, with set excitation at 512 nm; **c** time-dependence of the fluorescence anisotropy at 77 K, with excitation set at 403 nm and emission at 660 nm, for H_2TPPS^{4-} in protic and aprotic solvents: ethanol/methanol 3:2 (blue), d_4-methanol/deuterated water 98:2 (green), dimethylformamide/2-methyltetrahydrofuran/dichloromethane (orange) and dimethylformamide/acetonitrile (red)

initial value below $r=0.15$ followed by a fast decay in a time scale compared with the instrumental response function of ca. 0.4 ns. After that, the anisotropy reaches a plateau at values near $r=0.10$, which are stable in a time window of 20–25 ns corresponding to twice the lifetime. The plateau values slightly differ between protic and aprotic mixtures.

We collected and compared the FT-Raman spectra of H_2TPPS^{4-} and D_2TPPS^{4-} (Fig. 5) to get information on the vibrational modes coupled to the π-conjugated electronic transitions and verify the possible involvement of isotopic effects on vibronic couplings. Upon deuteration we observe just small variations in the FT-Raman spectra. This is consistent with the fact that only two hydrogens out of 26 are subject to isotopic substitution. Therefore, the perturbation induced on the vibrational structure is minor, producing its effects mainly in the region between 1250 and 1470 cm^{-1}. DFT simulations of the Raman spectra of H_2TPPS^{4-} and D_2TPPS^{4-} display the most evident variations in the same spectral region. Moreover, the peak shifts and intensity redistribution in the simulated spectra follow the experimental observation. Remarkably, the observed minor shift of peak A (Fig. 5a) is well reproduced by DFT calculations. The shift of this peak upon deuteration is justified by the presence of a sizeable NH bending contribution in the normal mode (Fig. 5b). Based on the Raman data, we may expect that vibronic couplings are just weakly affected by deuteration.

4 Discussion and conclusion

The aim of this work is to investigate in detail the phototautomerism in free-base porphyrins, with a specific focus on H_2TPPS^{4-}, based on preliminary results obtained by MPS [7]. Optical techniques, complementing EPR spectroscopy, have been exploited to gain insight into the process, while performing MPS experiments; they have been performed also in a deuterated solvent, enabling the exchange of the inner macrocycle protons to obtain D_2TPPS^{4-}.

Phototautomerism was early observed for H_2TPP by Zalesskii et al. [39] and by Völker et al. [11]. An elegant proof of its occurrence was provided by studying the absorption/emission of the molecules included in a *n*-octane Shpol'skii matrix at 77 K, where different tautomers occupying different inclusion sites are characterized by slightly different absorption spectra. To interpret the results Völker et al. invoked the presence of a proton libration around the out-of-plane axis involved in the vibronic-induced mixing of singlet and triplet states, so that the ISC occurs to an unrelaxed and distorted triplet structure, where the pyrrole protons are displaced toward the complementary pyrrole nitrogens. The nuclear relaxation of this structure populates the triplet state of both *trans* tautomers. It is well established that in free-base porphyrins the ISC is greatly enhanced in the presence of molecular distortion and a spin-vibronic coupling mechanism for ISC has been invoked [40]. This mechanism has been corroborated by relatively recent quantomechanical calculations [22].

H_2TPP and H_2TPPS^{4-} can be expected to behave similarly, as the sulphonate groups exert a modest effect on the optical transitions. Indeed, the Q-band absorption spectra of H_2TPP and of H_2TPPS^{4-} are almost overlapping in terms of maxima position and intensities, and the same holds for their emission spectra and for the fluorescence anisotropy measurements. Our measurements support the interpretation by Völker et al. [11]. Using MPS, we complete the picture by showing that an even distribution of the two *trans* tautomers is found at 77 K for H_2TPPS^{4-}, and the interconversion is slow within the relaxed triplet state. For D_2TPPS^{4-} slightly different weights are found. As for the role of the excited singlet state in the phototautomerization, information has been obtained from fluorescence anisotropy measurements.

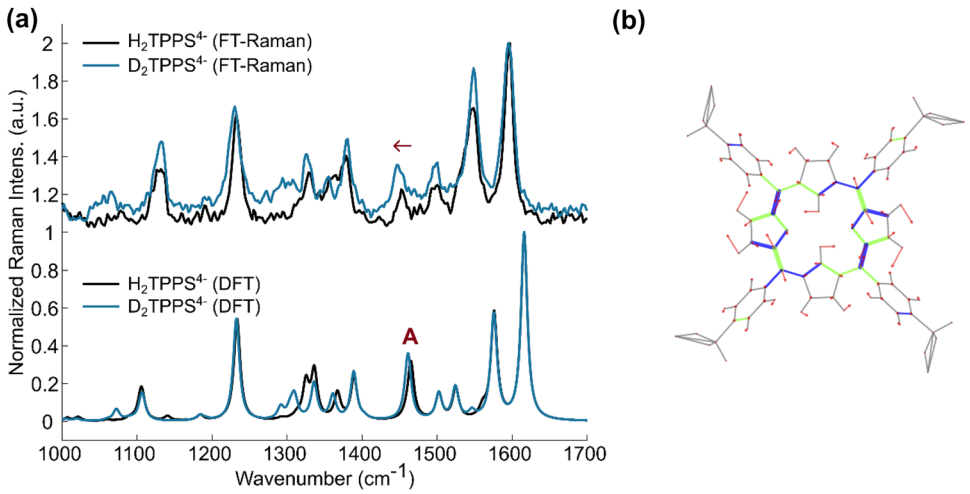

Fig. 5 **a** Experimental and simulated FT-Raman spectra of H_2TPPS^{4-} and D_2TPPS^{4-}; the peak marked with the letter "A" is assigned to the normal mode reported in panel (**b**), as computed by DFT on the fully hydrogenated molecule, and the arrow indicates the direction of its shift after deuteration; **b** representation of the marked normal mode (1494 cm^{-1}, 0 km/mol, 1431 A^4/amu), where the vectors of the nuclear displacements are indicated by red lines, and the bonds drawn with green (blue) lines are stretching (shrinking)

We have shown that, for H_2TPPS^{4-} in frozen solution, the anisotropy of the emission at 650 nm has its maximum value ($r = 0.25$) upon excitation of the $Q_x(0,0)$ band. Based on this result an efficient *trans–trans* phototautomerization in the excited singlet state, previously suggested to explain the MPS experiments [7], has been ruled out, as it would lead to $r = 0.1$. Combining the outcome of MPS and fluorescence anisotropy, excluding the direct involvement of the singlet excited state and of the corresponding triplet state, the central role of the spin-vibronic coupling mechanism for ISC in the phototautomerization is confirmed. In Fig. 6, we propose a scheme summarizing the model describing the photophysical/photochemical behaviour of H_2TPPS^{4-} with the focus on the *trans–trans* tautomerization process.

For H_2TPP in viscous solvent, in the absence of reorientational motion, Weigl [38] and Zalesskii [39] presented very similar r values, while the group of Waluk reported a value just below $r = 0.3$, in time-resolved mode (2 ps after a fs laser pulse), for excitation and emission near 650 nm [13]. However, in the same work, an inconsistency can be found with respect to the steady-state measurements, which were apparently obtained at room temperature in non-viscous solvent, showing a maximum value of 0.4 for the $Q_x(0,0)$ excitation [13]. The inconsistency is even stronger considering that for the bulkier derivative of H_2TPP, i.e. H_2TPPS^{4-}, which is characterized by a smaller rotational diffusion coefficient, we did not observe any fluorescence anisotropy at room temperature in analogous non-viscous solvents. It has been shown [38] that a high viscosity is required in order to exclude rotational depolarization in bulky porphyrins. Therefore, we raise doubts that a maximum value $r = 0.4$ can obtained for free-base porphyrins at room temperature.

To complete the critical analysis of the experimental data, we state that in the specific case of direct excitation of the

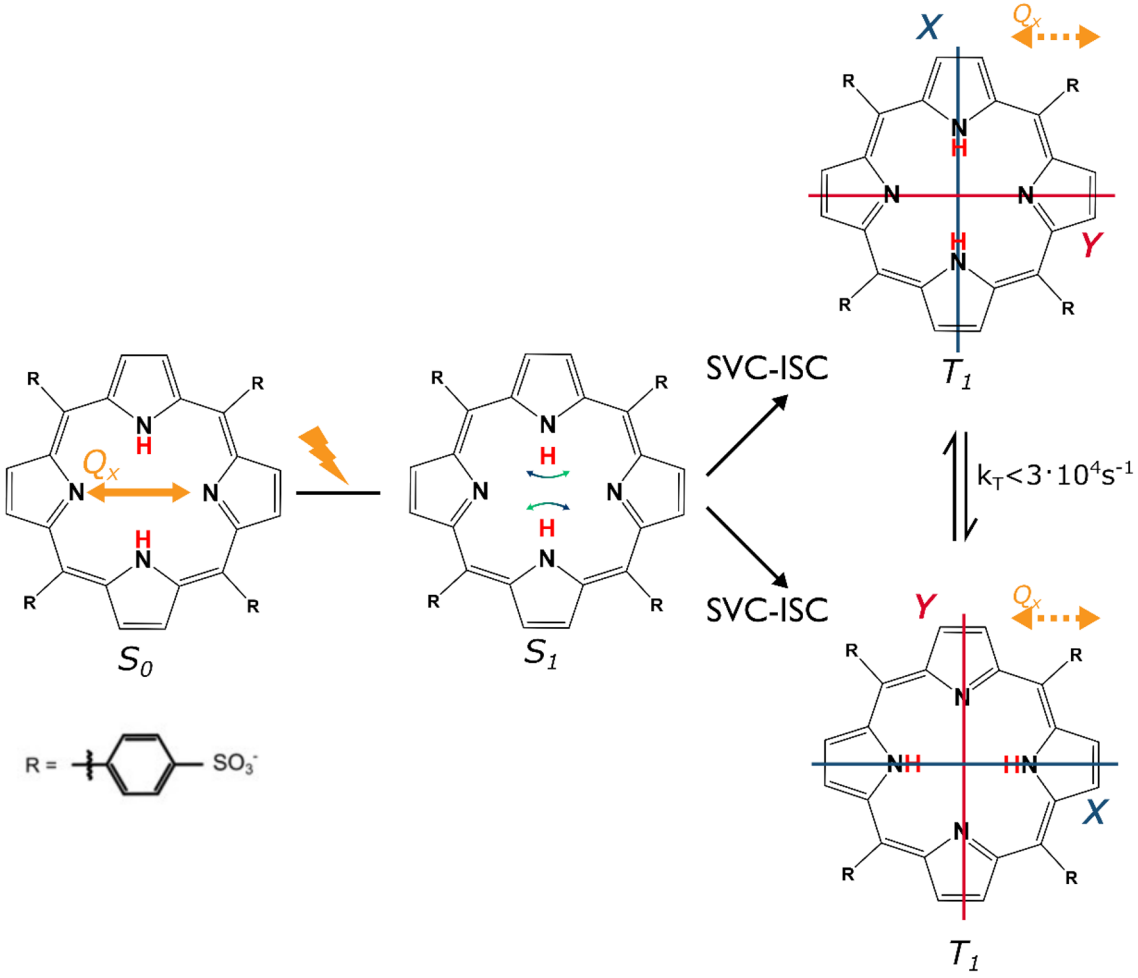

Fig. 6 Schematic representation of the *trans–trans* phototautomerization process for H_2TPPS^{4-}, promoted by a spin-vibronic coupling mechanism for ISC (SVC–ISC) and excitation of the Q_x transition (TDM represented by the solid yellow arrow). The vibrational motion of the inner protons (see Fig. 5b) is indicated by the green–blue arrows (the colours refer to the in-phase movement of the protons). The relative orientation of the TDM giving rise to photoselection (yellow dotted arrow)

Q_x(0,0) transition, the small depolarization effect observed ($r = 0.25$) is consistent with the presence of nearby vibronic states, having different directions of the TDM [41], that can be excited concomitantly to the Q_x(0,0) transition. We propose that the *trans–cis* tautomerization in the singlet excited state might be also responsible for some fluorescence depolarization. Indeed, the *cis* tautomer has been observed by TR-EPR as a minor component in the triplet spectrum. The spectral assignment to the *cis* tautomer is based on MPS simulations and on molecular symmetry reasoning, as reported in the result section. In the presence of an external heavy atom effect, this triplet is not observed anymore, supporting our hypothesis that the *trans–cis* tautomerization competes with the ISC and occurs in the singlet excited state. Moreover, our time-resolved fluorescence anisotropy exhibit a small decay that might be compatible with a kinetic process, not a quantum mechanical process.

As for the phototautomerization within the triplet state, instead, it can be demonstrated that the process is slow. The *trans–trans* tautomerization, where a switch of the position of the protons/deuterons between the occupied and vacant nitrogen positions happens, formally corresponds to an in-plane rotation by 90°. In the case of a fast process, the ZFS components along the *X* and *Y* axes would be completely averaged, therefore, the triplet state should be characterized by an orthorhombic tensor in the presence of molecular D_{2h} symmetry in the slow interconversion regime and by an axial tensor in case of higher D_{4h} symmetry in the fast interconversion regime. The analysis of the TR-EPR spectra for both H_2TPPS^{4-} and D_2TPPS^{4-} shows that the ZFS tensor is orthorhombic ($E \neq 0$), as determined for other free-base porphyrins [42], and the relative population rates of the *X* and *Y* triplet sublevels differ, which is consistent with a preserved D_{2h} symmetry for the molecule in the triplet state. We deduce that tautomerism in the excited triplet state occurs in the slow-motion regime both at 80 K and 105 K, which represents the upper temperature limit that we could reach to be able to work with a frozen solution while maintaining a good optical glass. Electron-Nuclear Double Resonance experiments on H_2TPPS^{4-} and on other free-base porphyrins are consistent with the TR-EPR results, confirming a D_{2h} symmetry in terms of proton hyperfine tensors [7, 43, 44]. A quantitative analysis of the data, reported in the Supporting Information, allows us to deduce that the first-order interconversion rate constant in the triplet state is $k_T < 3 \bullet 10^4 s^{-1}$.

Detailed analysis of the MPS experiments provides final confirmation on the phototautomerization process in free-base porphyrins. In our previous work [7], we have demonstrated that that a bimodal orientational distribution of the photoexcited molecules is required to obtain satisfactory simulations of TR-EPR spectra: the orientational distribution function is a sum of two orientational distribution functions, equally weighted, having each its own polarization axis, with the TDM parallel to the X and Y ZFS axes, respectively (see Fig. 6). This result is apparently inconsistent with the selective excitation of a single TDM during the TR-EPR experiment with polarized light, unless phototautomerization is invoked to explain the outcome of the simulations. After deuterium exchange of the central protons in D_2TPPS^{4-}, the ratio between the two TDM contributions in the orientational distribution changes and becomes uneven. In the first place, the isotopic substitution does not affect the quantum mechanical properties of the absorption processes, i.e. the electronic energy levels and the TDMs. Raman measurements provide very similar spectra for the two isotopically substituted molecules in the CC stretching region. Hence, it appears unlikely that the different TDM weights in H_2TPPS^{4-} and D_2TPPS^{4-} are correlated to excitation mechanisms of the π electrons that involve *significantly* different vibronic couplings for transitions near the fundamental Q_x(0,0). Nevertheless, the variation of the ratio between the two TDMs contributions depends on the temperature, which indicates the presence of a dynamic process sensitive to isotopic exchange. We assumed that the ISC process is assisted by a distortion of the structure that involves H (or D) displacements (Fig. 6). Such displacements are expected to be sensitive to the isotopic mass, which is indeed confirmed by the selective effect of the isotopic substitution on the Raman A peak that is assigned to the NH (ND) in-plane bending coupled with a collective CC stretching mode. This observation supports the interpretation of the MPS experiments in terms of phototautomerization.

It is worth to note that the weights of the TDMs contribution for D_2TPPS^{4-}, as obtained from MPS simulations, are coherent with the values obtained for the stationary fluorescence anisotropy: excitation on the Q_x(0,0) and Q_y(0,1) bands, where *r* was found to be positive, corresponds to a higher contribution from the Q_x TDM in the simulation. On the other hand, we obtained $r = -0.1$ upon excitation on the Q_y(0,0) band and correspondingly a higher contribution of the Q_y TDM is required in the MPS simulation. An almost 50:50 ratio is required when exciting on the Q_x(0,1), where $r \approx 0$ was found.

As a concluding remark, this spectroscopic work, aiming at the study of the phototautomerization of free-base porphyrins, has provided a model describing the photophysical/photochemical behaviour of H_2TPPS^{4-}. MPS is an important spectroscopic tool in the characterization of porphyrin excited states [45, 46] and a synergic approach based on magnetic and optical spectroscopy, with the aid of isotopic substitution, can provide a complete picture, linking together the first excited singlet state and the corresponding triplet state. We have proven that the *trans–trans* phototautomerization does not occur either in the excited singlet state or in the corresponding geometrically relaxed triplet state and our results support the interpretation that a spin-vibronic

coupling mechanism for ISC is responsible of the population of the two *trans* tautomers. As for the *trans–cis* phototautomerization, we have documented the formation of the *cis* conformer as an ancillary process in the singlet excited state. The results obtained for H_2TPPS^{4-} can be extended to the entire class of free-base porphyrins and provide key information on the excited state electronic structure, with important implications in terms of photochemical stability and reactivity. Unravelling the details of the photophysics/photochemistry of porphyrins is a fundamental requisite to improve biomimetic systems based on this important class of molecules.

Supplementary Information The online version contains supplementary material available at https://doi.org/10.1007/s43630-023-00413-5.

Acknowledgements The authors acknowledge the Department of Chemical Sciences of the University of Padova (Nexus project) and the Interdepartmental Centre Giorgio Levi Cases for Energy Economics and Technology (Biomolecular DSSCs Project) for financial support.

Funding Open access funding provided by Università degli Studi di Padova within the CRUI-CARE Agreement. Università degli Studi di Padova, Interdepartmental Centre Giorgio Levi Cases for Energy Economics, Marilena Di Valentin, Technology (Biomolecular DSSCs Project), Marilena Di Valentin, Project Nexus,Antonio Barbon.

Data Availability The authors declare that the data supporting the findings of this study are available within the paper and its Supplementary Information files. Should any raw data files be needed in another format they are available from the corresponding author upon reasonable request.

Declarations

Conflict of interest There are no conflicts of competing interest to declare.

References

1. Dolphin, D. (1978). *The Porphyrins*. Academic Press.
2. Fraser, C. L., & Smith, A. P. (2003). Fundamentals: Ligands, Complexes, Synthesis, Purification, and Structure. *Comprehensive coordination chemistry II: from biology to nanotechnology.* Amsterdam: Elsevier.
3. Min Park, J., Lee, J. H., & Jang, W.-D. (2020). Applications of porphyrins in emerging energy conversion technologies. *Coordination Chemistry Reviews, 407*, 213157. https://doi.org/10.1016/j.ccr.2019.213157
4. Senge, M. O., Fazekas, M., Notaras, E. G. A., Blau, W. J., Zawadzka, M., Locos, O. B., & Ni Mhuircheartaigh, E. M. (2007). Nonlinear optical properties of porphyrins. *Advanced Materials, 19*(19), 2737–2774. https://doi.org/10.1002/adma.200601850
5. Farjtabar, A., & Gharib, F. (2010). Solvent effect on protonation constants of 5, 10, 15, 20-Tetrakis(4-sulfonatophenyl)porphyrin in different aqueous solutions of methanol and ethanol. *Journal of Solution Chemistry, 39*(2), 231–244. https://doi.org/10.1007/s10953-010-9496-y
6. Improta, R., Ferrante, C., Bozio, R., & Barone, V. (2009). The polarizability in solution of tetra-phenyl-porphyrin derivatives in their excited electronic states: A PCM/TD-DFT study. *Physical Chemistry Chemical Physics, 11*(22), 4664. https://doi.org/10.1039/b902521a
7. Barbon, A., Dal Farra, M. G., Ciuti, S., Albertini, M., Bolzonello, L., Orian, L., & Di Valentin, M. (2020). Comprehensive investigation of the triplet state electronic structure of free-base 5,10,15,20-tetrakis(4-sulfonatophenyl)porphyrin by a combined advanced EPR and theoretical approach. *The Journal of Chemical Physics, 152*(3), 034201. https://doi.org/10.1063/1.5131753
8. Hashimoto, T., Choe, Y.-K., Nakano, H., & Hirao, K. (1999). Theoretical study of the Q and B bands of free-base, magnesium, and zinc porphyrins, and their derivatives. *The Journal of Physical Chemistry A, 103*(12), 1894–1904. https://doi.org/10.1021/jp984807d
9. Minaev, B., & Lindgren, M. (2009). Vibration and fluorescence spectra of porphyrin- coredbis(methylol)-propionic acid dendrimers. *Sensors, 9*(3), 1937–1966. https://doi.org/10.3390/s90301937
10. Lopes, J. M. S., Sampaio, R. N., Ito, A. S., Batista, A. A., Machado, A. E. H., Araujo, P. T., & Neto, N. M. B. (2019). Evolution of electronic and vibronic transitions in metal(II) meso-tetra(4-pyridyl)porphyrins. *Spectrochimica Acta Part A: Molecular and Biomolecular Spectroscopy, 215*, 327–333. https://doi.org/10.1016/j.saa.2019.02.024
11. Völker, S., & van der Waals, J. H. (1976). Laser-induced photochemical isomerization of free base porphyrin in an *n* -octane crystal at 4·2 K. *Molecular Physics, 32*(6), 1703–1718. https://doi.org/10.1080/00268977600103021
12. Yu, H.-Z., Baskin, J. S., & Zewail, A. H. (2002). Ultrafast dynamics of porphyrins in the condensed phase: II. zinc tetraphenylporphyrin. *The Journal of Physical Chemistry A, 106*(42), 9845–9854. https://doi.org/10.1021/jp0203999
13. Białkowski, B., Stepanenko, Y., Nejbauer, M., Radzewicz, C., & Waluk, J. (2012). The dynamics and origin of the unrelaxed fluorescence of free-base tetraphenylporphyrin. *Journal of Photochemistry and Photobiology A: Chemistry, 234*, 100–106. https://doi.org/10.1016/j.jphotochem.2011.10.026
14. Yeon, K. Y., Jeong, D., & Kim, S. K. (2010). Intrinsic lifetimes of the Soret bands of the free-base tetraphenylporphine (H2TPP) and Cu(ii)TPP in the condensed phase. *Chemical Communications, 46*(30), 5572. https://doi.org/10.1039/c0cc01115k
15. de Souza, T. G. B., Vivas, M. G., Mendonça, C. R., Plunkett, S., Filatov, M. A., Senge, M. O., & De Boni, L. (2016). Studying the intersystem crossing rate and triplet quantum yield of *meso* -substituted porphyrins by means of pulse train fluorescence technique. *Journal of Porphyrins and Phthalocyanines, 20*(44), 282–291. https://doi.org/10.1142/S1088424616500048
16. Braun, J., Koecher, M., Schlabach, M., Wehrle, B., Limbach, H.-H., & Vogel, E. (1994). NMR study of the tautomerism of porphyrin including the kinetic HH/HD/DD isotope effects in the liquid and the solid state. *Journal of the American Chemical Society, 116*(15), 6593–6604. https://doi.org/10.1021/ja00094a014

17. Ribó, J. M., Farrera, J.-A., Valero, M. L., & Virgili, A. (1995). Self-assembly of cyclodextrins with meso-tetrakis(4-sulfonatophenyl)porphyrin in aqueous solution. *Tetrahedron, 51*(12), 3705–3712. https://doi.org/10.1016/0040-4020(95)00085-M
18. Zalesskii, I. E., Kotlo, V. N., Sevchenko, A. N., Solov'ev, K. N., & Shkirman, S. F. (1973). Time dependence of fluorescence polarization for porphyrins and displacement of the imino hydrogen in the porphyrin ring. *Soviet Physics Doklady, 17*, 1183.
19. Radziszewski, J. G., Waluk, J., & Michl, J. (1989). Site-population conserving and site-population altering photo-orientation of matrix-isolated free-base porphine by double proton transfer: IR dichroism and vibrational symmetry assignments. *Chemical Physics, 136*(2), 165–180. https://doi.org/10.1016/0301-0104(89)80044-8
20. Uttamlal, M., & Sheila Holmes-Smith, A. (2008). The excitation wavelength dependent fluorescence of porphyrins. *Chemical Physics Letters, 454*(4–6), 223–228. https://doi.org/10.1016/j.cplett.2008.02.012
21. Zagusta, G. A., Kotlo, V. N., & ShkirmanSolov'ev, S. F. K. N. (1977). Dependence of the degree of fluorescence polarization of porphyrins on the time of photoexcitation and temperature. *Journal of Applied Spectroscopy, 27*(1), 946–947. https://doi.org/10.1007/BF00619048
22. Perun, S., Tatchen, J., & Marian, C. M. (2008). Singlet and triplet excited states and intersystem crossing in free-base porphyrin: TDDFT and DFT/MRCI Study. *ChemPhysChem, 9*(2), 282–292. https://doi.org/10.1002/cphc.200700509
23. Solov'ev, K. N., & Shkirman, S. F. (1993). Photoinduced NH-tautomerism and vibronic states of hydroporphyrin molecules. *Journal of Applied Spectroscopy, 58*(1–2), 29–35. https://doi.org/10.1007/BF00659156
24. Waluk, J. (1999). Light-induced tautomerization in porphyrin isomers. *Acta Physica Polonica A, 95*(1), 49–62.
25. Kay, C. W. M., Elger, G., & Möbius, K. (1999). The photoexcited triplet state of free-base porphycene: a time-resolved EPR and electron spin echo investigation. *Physical Chemistry Chemical Physics, 1*(17), 3999–4002. https://doi.org/10.1039/a903382c
26. Kay, C. W. M., Gromadecki, U., Törring, J. T., & Weber, S. (2001). An investigation of the structure of free-base porphycene by time-resolved electron nuclear double resonance and density functional theory on the photoexcited triplet state. *Molecular Physics, 99*(16), 1413–1420. https://doi.org/10.1080/00268970110054520
27. Naoum, M. M., & Saad, G. R. (1988). Solvent effect on tautomeric equilibria and dipole moments of some alpha substituted benzoylacetanilides. *Journal of Solution Chemistry, 17*(1), 67–76. https://doi.org/10.1007/BF00651854
28. Campos, R. B., Silva, V. B., Menezes, L. R. A., Ocampos, F. M. M., Fernandes, J. M., Barison, A., & Orth, E. S. (2020). Competitive reactivity of tautomers in the degradation of organophosphates by imidazole derivatives. *Chemistry A European Journal, 26*(22), 5017–5026. https://doi.org/10.1002/chem.201905379
29. Van Hook, A. W. (2011). Isotope effects in chemistry. *Nukleonika, 56*(3), 217–240.
30. Toffoletti, A., Wang, Z., Zhao, J., Tommasini, M., & Barbon, A. (2018). Precise determination of the orientation of the transition dipole moment in a Bodipy derivative by analysis of the magnetophotoselection effect. *Physical Chemistry Chemical Physics, 20*(31), 20497–20503. https://doi.org/10.1039/C8CP01984C
31. Tait, C. E., Neuhaus, P., Anderson, H. L., & Timmel, C. R. (2015). Triplet state delocalization in a conjugated porphyrin dimer probed by transient electron paramagnetic resonance techniques. *Journal of the American Chemical Society, 137*(20), 6670–6679. https://doi.org/10.1021/jacs.5b03249
32. Redman, A. J., Moise, G., Richert, S., Peterson, E. J., Myers, W. K., Therien, M. J., & Timmel, C. R. (2021). EPR of photoexcited triplet-state acceptor porphyrins. *The Journal of Physical Chemistry C, 125*(21), 11782–11790. https://doi.org/10.1021/acs.jpcc.1c03278
33. Barbon, A., & Brustolon, M. (2012). An EPR study on nanographites. *Applied Magnetic Resonance, 42*(2), 197–210. https://doi.org/10.1007/s00723-011-0285-6
34. Stoll, S., & Schweiger, A. (2006). EasySpin, a comprehensive software package for spectral simulation and analysis in EPR. *Journal of Magnetic Resonance, 178*(1), 42–55. https://doi.org/10.1016/j.jmr.2005.08.013
35. M. J. Frisch, G. W. Trucks, H. B. Schlegel, G. E. Scuseria, M. A. Robb, J. R. Cheeseman, G. Scalmani, V. Barone, B. Mennucci, G. A. Petersson, H. Nakatsuji, M. Caricato, X. Li, H. P. Hratchian, A. F. Izmaylov, J. Bloino, G. Zheng, J. L. Sonnenberg, M. Hada, M. Ehara, K. Toyota, R. Fukuda, J. Hasegawa, M. Ishida, T. Nakajima, Y. Honda, O. Kitao, H. Nakai, T. Vreven, J. A. Montgomery, Jr., J. E. Peralta, F. Ogliaro, M. Bearpark, J. J. Heyd, E. Brothers, K. N. Kudin, V. N. Staroverov, T. Keith, R. Kobayashi, J. Normand, K. Raghavachari, A. Rendell, J. C. Burant, S. S. Iyengar, J. Tomasi, M. Cossi, N. Rega, J. M. Millam, M. Klene, J. E. Knox, J. B. Cross, V. Bakken, C. Adamo, J. Jaramillo, R. Gomperts, R. E. Stratmann, O. Yazyev, A. J. Austin, R. Cammi, C. Pomelli, J. W. Ochterski, R. L. Martin, K. Morokuma, V. G. Zakrzewski, G. A. Voth, P. Salvador, J. J. Dannenberg, S. Dapprich, A. D. Daniels, O. Farkas, J. B. Foresman, J. V. Ortiz, J. Cioslowski, and D. J. Fox, Gaussian, Inc., Wallingford CT, 2013.
36. Bukartė, E., Haufe, A., Paleček, D., Büchel, C., & Zigmantas, D. (2020). Revealing vibronic coupling in chlorophyll c1 by polarization-controlled 2D electronic spectroscopy. *Chemical Physics, 530*, 110643. https://doi.org/10.1016/j.chemphys.2019.110643
37. Bolzonello, L., Albertini, M., Collini, E., & Di Valentin, M. (2017). Delocalized triplet state in porphyrin J-aggregates revealed by EPR spectroscopy. *Phys Chem Chem Phys PCCP, 19*(40), 27173–27177. https://doi.org/10.1039/C7CP02968C
38. Weigl, J. W. (1957). The polarization of the fluorescence of tetraphenylporphine. *Journal of Molecular Spectroscopy, 1*(1–4), 133–138. https://doi.org/10.1016/0022-2852(57)90016-4
39. Zalesskii, I. E., Kotlo, V. N., Solovev, K. N., & Shkirman, S. F. (1974). Polarization spectra of metalloporphyrins. *Journal of Applied Spectroscopy, 20*(6), 761–764. https://doi.org/10.1007/BF00614152
40. Penfold, T. J., Gindensperger, E., Daniel, C., & Marian, C. M. (2018). Spin-vibronic mechanism for intersystem crossing. *Chemical Reviews, 118*(15), 6975–7025. https://doi.org/10.1021/acs.chemrev.7b00617
41. Lopes, J. M. S., Sharma, K., Sampaio, R. N., Batista, A. A., Ito, A. S., Machado, A. E. H., & Barbosa Neto, N. M. (2019). Novel insights on the vibronic transitions in free base meso-tetrapyridyl porphyrin. *Spectrochimica Acta Part A: Molecular and Biomolecular Spectroscopy, 209*, 274–279. https://doi.org/10.1016/j.saa.2018.10.054
42. van Dorp, W. G., Soma, M., Kooter, J. A., & van der Waals, J. H. (1974). Electron spin resonance in the photo-excited triplet state of free base porphin in a single crystal of *n* -octane. *Molecular Physics, 28*(6), 1551–1568. https://doi.org/10.1080/00268977400102801
43. Kay, C. W. M. (2003). The electronic structure of the photoexcited triplet state of free-base (tetraphenyl)porphyrin by time-resolved electron−nuclear double resonance and density functional theory. *Journal of the American Chemical Society, 125*(45), 13861–13867. https://doi.org/10.1021/ja036278j
44. Kay, C. W. M., Di Valentin, M., & Möbius, K. (1995). A time-resolved electron nuclear double resonance (ENDOR) study of the photoexcited triplet state of free-base tetraphenylporphyrin. *Solar Energy Materials and Solar Cells, 38*(1–4), 111–118. https://doi.org/10.1016/0927-0248(94)00219-3

45. Ciuti, S., Barbon, A., Bortolus, M., Agostini, A., Bergantino, E., Martin, C., & Carbonera, D. (2021). Neuroglobin provides a convenient scaffold to investigate the triplet-state properties of porphyrins by time-resolved epr spectroscopy and magnetophotoselection. *Appl Mag Res*. https://doi.org/10.1007/s00723-021-01421-3

46. Ciuti, S., Agostini, A., Barbon, A., Bortolus, M., Paulsen, H., Di Valentin, M., & Carbonera, D. (2022). Magnetophotoselection in the investigation of excitonically coupled chromophores: the case of the water-soluble chlorophyll protein. *Molecules, 27*(12), 3654. https://doi.org/10.3390/molecules27123654